AIAA 97-3874

Analysis of Conception of a Gas-Loaded Variable Conductance Capillary Pumped Loop

V.V.Vlassov
INPE, National Institute for Space Research
S.J.Campos, SP, Brazil

1997 National Heat Transfer Conference

Baltimore, MD
August 10 - 12, 1997

ANALYSIS OF CONCEPTION OF A GAS-LOADED VARIABLE CONDUCTANCE CAPILLARY PUMPED LOOP

Valeri V. Vlassov

National Institute for Space Research - INPE, S.J.Campos, SP, Brazil.

The theoretical investigation was being conducted to look into possibility to provide passive control in capillary pumped loops (CPL) using the non-condensable gas technique. The principal condition to apply the gas-control technique for CPL is condenser of the wicked type. Corresponding designs of cylindrical porous condenser and evaporator as well are proposed. The developed mathematical model of entire system combines the hydrodynamic and heat transfer sections. This combination allows the tracking of position of interfaces in the both wicks. Various aspects are analyzed: priming, dry-out, start-up, conditions for vapor bubble formation and collapse. Also the hazard of gas penetration in liquid phase is discussed. Performed examination of the conception confirms possibility to develop a CPL with porous condenser and non-condensable gas reservoir for passive control of heat transport capability.

Nomnclature

A	= Area	m^2
C	= Specific heat	$J\ kg^{-1}\ K^{-1}$
G	= Thermal conductance	$W\ K^{-1}$
K	= Permeability	m^2
L	= Length	m
P	= Pressure	Pa
R	= Gas constant	$J\ kmole^{-1}\ K^{-1}$
S	= Perimeter	m
T	= Temperature	K
V	= Volume	m^3
Y	= Coordinate	m
Z	= Coordinate	m
a	= Form factor	?
g	= Gravitation	$m\ s^{-2}$
h	= Height	m
k	= Thermal conductivity	$Wm^{-1}K^{-1}$
l	= Liquid	m
m	= Mass flow rate	$kg\ s^{-1}$
m	= Mass	kg
q	= Heat flux density	Wm^{-2}
r	= Radius	m
t	= Thickness	m
u	= Velocity	$m\ s^{-1}$
x	= Recession	m
α	= Accomodation coefficient	-
δ	= Variation	
δ	= Logic function (0,1)	-
ε	= Porosity	
ε	= Emissivity	
η	= Fin efficiency factor	
φ	= Portion of length	-
λ	= Latent heat	$J\ kg^{-1}$
μ	= Dynamic viscosity	Pa s
θ	= Wetting angle	rad
ρ	= Density	$kg\ m^{-3}$
σ	= Surface tension	$N\ m^{-1}$
σ	= Stefan-Boltzman constant	$WK^{-4}m^{-2}$
τ	= Time	s
ξ	= Friction factor	

Subscripts:

a	= Active
c	= Condenser
e	= Evaporator
eff	= Effective
ext	= External
f	= Fluid
g	= Gas
i	= Interface
in	= Inactive
l	= Liquid
p	= Pore
r	= Reservoir
rad	= Radiator
s	= Surface
sat	= Saturated
t	= Total
v	= Vapor
w	= Wall
z	= Coordinate along length
1	= Inlet
2	= Outlet

Introduction

Heat transportation for relatively long distances is a necessity in many engineering practical application. The simplest approach is to organize heat exchange with pumped media, usually liquid or gas. Using phase change (liquid/vapor) during heat acquisition or releasing allows drastically decreasing

total mass flow rate in the order of ratio between latent heat of vaporization and specific heat. Even capillary pressure can be enough to pump liquid instead of electrical-mechanical pumps in single-phase systems.

Capillary pumping principle has been realized in heat pipes. No external energy is needed to put this device in action except applied heat itself. The heat pipe really is a passive superconductor of heat, due to the effective thermal resistance is of two order of magnitude less with compare of solid tube of the same dimension, made from the metal of best conductivity - pure silver.

Alternative heat pipe designs differ with capillary structure, material and work fluids. For all modifications of canonical heat pipes, the maximum capacity is limited mainly by hydraulic resistance of liquid return through the porous media along full length of the pipe.

The principle of liquid flow bypassing of porous media has been realized in arterial heat pipes and recently, in mono-groove ones. Farther extension of the bypassing idea has found in the principle of complete separation of phase streams.

A capillary pumped loop (CPL) represent a heat transport device used mentioned principle. Basically the CPL consists of evaporator with porous media, two separate tubes for vapor and liquid, and condenser. Stenger (1966)[16] developed one of the first laboratory prototypes of CPL.

In general, CPL has conditions to reach much higher values of heat transport capability in contradistinction of canonical heat pipes. The principle of separation of streams give ability to use very small pore size to provide high capillary head in the evaporator and low hydraulic resistance in the liquid line.

Gravity forces can affect seriously the performance of any capillary pumped devices up to break in operation. In contradistinction, 0-g conditions provide perfect environment for operation. Therefore, space application in spacecraft thermal control is matched completely of the nature of capillary pumped devices.

The CPLs are very attractive for satellite thermal control. They have much higher heat transport characteristic and they are not so sensitive to body force fluctuations (caused, for example, by orbital maneuvers of satellite). Also CPLs have more flexibility to adjust in the satellite layout than heat pipes. The vapor or liquid line can be bent as an electrical cable, due to no existence of wick inside them. The CPL conception has very big potential to be expanded to a complex multi branch capillary pumped system with several evaporators and condensers.

In fact, few flight tests of CPL were realized up to now and the CPLs are under the investigation at the present.

Problems of control

Space environment provides very external thermal conditions for capillary pumped device operation. Effective temperature of heat sink can be varied from 60 up to 400 oK during one orbit. Source heat loads also can be varied from 0 up to 100% of defined level. At the same time required range of source temperature variation usually restricted by difference of 20-40oK. This fact calls the necessity of development of capillary pumped devices with variable thermal resistance.

There are two different approaches to control accomplishing. First one is active approach with using of additional electric heater controlled by electronics. Second one is passive self-control, without using of any additional electronics and other kind of energy except of heat. First approach can provide very precision control of source temperature, and second one is more preferable from position of weight, electric power consumption penalty and complexity, cost and reliability as well.

Non-condensable gas conception is widely used for control purposes in heat pipes. It is realized by linking of an additional gas reservoir to the end of condenser zone. Diffusion front between gas and vapor provide particular blockage of condensation area, decreasing effective area for heat removal. This front is moved in response of variation in sink and source conditions, providing the control of variable effective area mode. If volume of reservoir is more than volume of vapor channel of the condenser, it is possible to provide effective and passive self-control. Application of heater controlled by electronic to the reservoir (active approach) gives possibility to improve stability of source temperature and allow reducing the volume of the reservoir.

Some other principles of passive control exist, like liquid blockage technique and by change of hydraulic resistance of vapor flow by an orifice controlled mechanically by a bellow. But these techniques did not find application in Space.

Control technique for CPL usually restricted by active approach by changing of set point of reservoir to support a saturation pressure in the evaporator zone. Liquid storage reservoir is connected to the liquid line for compensation the liquid volume change because of movement of liquid/vapor interface in the tube-type condenser. Also this reservoir supplies the liquid to the evaporator during start-up.

Alternative passive approaches, recently published, include bypass technique using a bellow as self-controlled mechanical regulator, and freezable condenser.

Existing technique for active control based on tube-type conception of condenser with moving interface between liquid and vapor. Thus, in reality, area of the condenser is like divided in two parts: two-phase and liquid one. The pressure and temperature in the inlet zone of the condenser are supported at approximately the same level of evaporator zone by active regulation of reservoir. Due to relatively low value of mass flow rate, the temperature of liquid phase falls down rapidly along length of the tube. Thus, it looks like liquid blockage technique realized with active control.

Conception of tube type condenser showed some problems of possible vapor phase appearance in liquid line under high heat loads. This method of control can provide also some pressure oscillation [7,9], related with presence of two-phase reservoir for flooding the condenser with liquid.

Passive control technique with non-condensable gas in porous condenser has been successfully demonstrated in a two-phase mechanically pumped system of high heat transfer capacity. Pressure has been controlled by feedback valves, and the gas has been loaded to condenser only after completely wetting of capillary structure with liquid and putting the CPL in operation without gas (the mode of gas loading after start-up).

Existing techniques of passive control in CPL are based on the same tube type conception of condenser. Presence of bellow-type regulator can decrease the reliability of the system. The freezing condenser conception has worst transient characteristics, because the time constant will include time for secondary phase transmission (solid-liquid). Wherefore, the quest for alternative methods of passive control has to be continued.

Conception of gas loaded CPL

Successful application of non-condensable technique of passive control in variable conductance heat pipes (VCHP) gives a premise for the analysis of possibility of utilization of this technique to CPL.

Method of gas control in a CPL can be accomplished only in conditions of wicked type condenser.

Some conceptions CPL with wicked condenser already have been developed. One of them is known as thermal power loop. Prototypes show operational characteristics as a device of constant conduction.

A laboratory prototype of CPL with flat porous wicks in evaporator and condenser has been successful tested in 1996[19].

The proposed design of the CPL consists of cylindrical evaporator, cylindrical wicked condenser of similar external shape and a gas reservoir

The condenser of proposed conception of CPL (Fig. 1) consists of an axial grooved tube and inserted porous structure, covering these channels of the tube. Grooves and screen wick serve for liquid storage, and central core of the tube is occupied by vapor-gas mixture. This condenser looks like canonical HP with composite wick, combined with axial grooves and covering with porous screen. A saddle is used to provide a good thermal connection between external wall of the tube and flat surface of a space radiator.

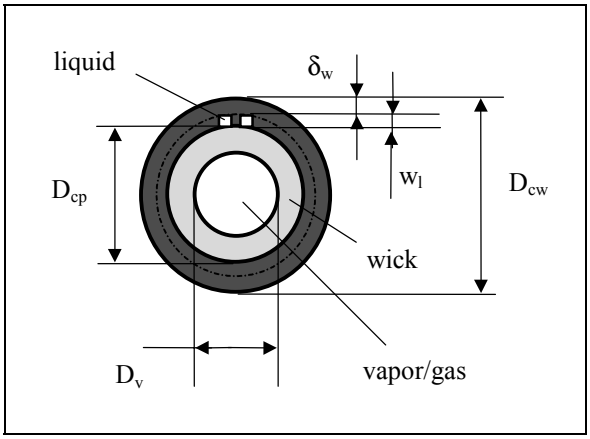

Fig. 1. Conception of the CPL wick condenser design

Cylindrical evaporator (Fig.2) has sintered powder structure and axial/circular grooves to collect vapor phase. The central core is used for liquid supply of the wick.

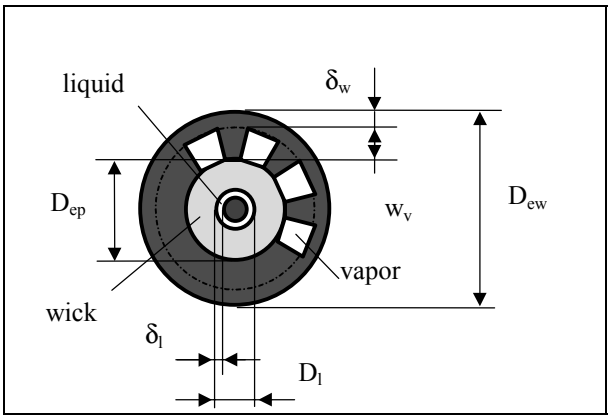

Fig. 2. The CPL evaporator design.

A metallic pin is inserted into the liquid channel to provide capillary conditions for self-priming: $\delta_l < w_v$.

Both the evaporator and the condenser have the similar design with mirror phase distribution. The distinction lays in dimensions of the channels, those have to be different to accommodate the alteration in liquid and vapor densities.

Based CPL design has following geometric parameters.

Evaporator: D_{ew}=32mm; L_e=80mm; D_{ep}=20mm; w_v=3mm; δ_w=2mm; D_l=5mm; δ_l=1mm; r_e=20μm; K_e=1.2e-10; ε_e=0.32; $\theta' = 8^0$.

Condenser: D_{cw}=30mm; L_c=180mm; D_{cp}=20mm; w_l=1mm; δ_w=2mm; D_v=8mm; r_c=60μm; K_c=5.6e-10; ε_c=0.40; $\theta' = 8^0$; A_{rad}=0.15m2; η_{rad}=0.8; ε_{rad}=0.9.

Reservoir and communications: V_r=30cm^3; L_l=0.6m; D_l=1mm; L_v=2m; D_v=4mm. Type of the reservoir: wicked or unwicked. Reservoir coupling: cold or hot or insulated.

Construction material is aluminum; material for wick - sintered powder nickel or titanium; working fluid - ammonia; non-condensable gas - nitrogen.

A reservoir with non-condensable gas is linked to core of condenser tube to provide the self-control by movement of diffusion front between vapor and gas. The reservoir can be of wicked or unwicked type. In case of wicked reservoir, the addition communication link for liquid phase between wicks of the reservoir and of condenser should be established.

The CPL design is sized to satisfy the conditions of self-priming, which will be discussed in the next section. It means that in conditions of presence of two phases only the phases will be properly separated before start-up.

The presence of gas in liquid phase in general can blockage the evaporator and break the operation of CPL. To minimize this hazard, the technique of gas loading after start-up should be utilized. It can be accomplished by installation of additional valve in the communication line between the reservoir and vapor core of the condenser. This valve can be actuated by telecommand, after successful start-up in the ordinary CPL mode.

Non-condensable gas bubbles can appear in the liquid section with time due to releasing of the gas dissolved in work liquid or accidentally after dry-out of wick. This is a reason that the design probably shall include a bubble trap appendix from evaporator side. Gas bubbles move with liquid trough the entire evaporator to the end and when are stored in the trap due to conical shape of the pin, inserted to the liquid channel (duct) of the evaporator.

Blow-off vapor from the trap needs a special proceeding. It includes stop of CPL operation and forced vaporization of liquid from the trap wick. Heating this thin wick with electric heater will cause dry-out of it. After that gas, collected in the trap, can penetrate the wick and blow out to the vapor duct.

The porous wick of the trap should be of good conductivity and of small thickness with compare to one of the evaporator.

The gas trap adds to CPL complexity but it is the price for self-control ability. Final decision for selection optimal design has to be based on the complete analysis of performance of gas-controlled CPL.

Priming

The design of CPL must provide conditions for proper phase distribution before and during start-up. In this gas-load conception it is assumed that non-condensable gas will be loaded to condenser only after proper start-up with vapor/liquid mixture. After complete wetting of capillary structure in the condenser, a valve in gas feed line has to be open to load gas.

One of the main problems of CPL is to put it in proper mode of operation. This problem is more critical in the CPLs than in the heat pipes, due to unpredictable initial phase distribution inside the CPL in general case. No established way of start-up exists at the present. Several investigations have been done on this subject. It is possible to supply the evaporator with the liquid initially stored in the reservoir In the CAPL2 experiment a special starter than is used to flush out liquid from vapor line before switch-on the heat load. In CPL without separated reservoir, known as loop HP (LHP), a special profile of heat loading is applied to guaranty an initially large difference in the conditions above and below of evaporator wick.

Another option to have a successful start-up is to size the CPL in a way to guarantee a proper phase distribution, using the capillary forces. This approach is found to be convenient for the present design of CPL with wicked condenser.

In this case, the proper phase distribution means liquid and vapor phase totally separated. Considering a qualitative analysis, to avoid vapor bubble at the liquid voids, it is necessary to guaranty that all spaces in this part of CPL were smaller than the voids, assigned for vapor phase. This condition provides a capillary force to suck liquid to the smaller voids.

The conditions for initial proper phase distribution, for this prototype, may be extracted from the balance of capillary forces between the base plate grooves and the liquid line. The involved parameters are shown in Fig. 3.

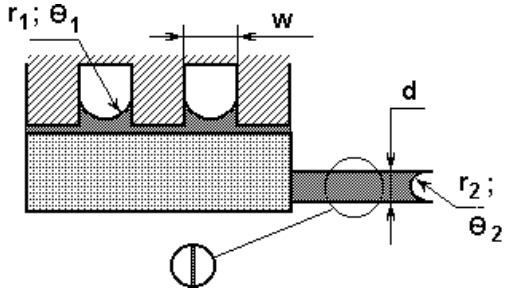

Fig.3. Capillary conditions for self-priming

The capillary forces can prevent the formation of vapor bubble in the liquid line if the following expression is true:

$$\frac{2\sigma\cos\theta_1}{w} < \frac{4\sigma\cos\theta_2}{d} \qquad (1)$$

During the CPL operation, the prevention of bubble formation in the liquid line is also very important. The prevention is done using the subcooling of the liquid in the condensation. The subcooling acts against the disjoint pressure that can change the local saturation conditions and thus break the liquid continuity. The disjoint pressure is higher in wicked condenser than in ordinary tube-type condenser and depends on the amount of charge and operation conditions.

The necessary subcooling ΔT can be found from the expression:

$$\Delta T > \frac{2T\sigma\cos\theta}{\lambda\rho_v r_p} \qquad (2)$$

Following preliminary practical recommendations for the design may be extracted:

- slight overfilling of the CPL is better than underfilling;
- it is better to use a coarse mesh in the condenser;
- it is necessary to provide conditions in the condenser for subcooling of liquid.

The conditions for subcooling is met automatically for the condenser design, shown in the Fig.1

Mathematical model

Analysis of the CPL as a system can be accomplished by simulation of behavior on system level rather that study separated processes of phase transmission in porous elements and flow in channels. For the CPL it is important to link thermal and hydrodynamic models to estimate so important integral transient characteristics like start-up, control ability, dry-out, interfaces movements.

The main assumptions of the model:

- Flat one-dimensional front at the gas/vapor interface
- The evaporation and condensation rates and temperatures are uniform within prescribed regions.
- No mass and heat diffusion through the gas/vapor front.
- The gas in the reservoir is in the heat equilibrium with reservoir wall.
- Vapor is in the saturated condition in the vapor ducts.

The capillary forces play a key role in any capillary-drive heat transfer device. Let suggest for the present analysis the model of a capillary structure as a set of capillaries with predicted radius r_i.

There are several mechanisms of changing in curvature of meniscus. First one is due to change in mass balance on interface between of liquid arrived from wick bulk and vapor flow removed by evaporation. This mechanism is important for describing of initial stage of the dry-out process in an evaporator wick when deficit of liquid supply to the interface occurs. Practically it can be happened due to: 1) high evaporation rate (capillary limit); 2) gravity fluctuations in adverse direction of liquid flow; 3) viscosity increasing in conditions of cold condenser and high heat loading of evaporator; 4) change of liquid inventory via change of the balance between total masses of vapor and liquid phases in reply of change of environment conditions.

Micro variation of volume of liquid in a capillary can be described via variation of the angle of contact:

$$\delta V = -\rho\pi r^3 \Phi'(\Theta)\delta\Theta \qquad (3)$$

Where

$$\Phi(\Theta) = \frac{(1-sin\Theta)^2(2+sin\Theta)}{\cos^3\Theta} \qquad (4)$$

The curvature of meniscus can be changed until the critical angle of contact θ‘ is reached. After that the recession of the interface begins with constant angle of meniscus curvature. Overall system for interface movement for evaporator and condenser wicks can be expressed via terms of wetting angle and meniscus recession x:

$$\begin{aligned} \varepsilon_e A_e\left[r_e\Phi'(\Theta_e)\frac{d\Theta_e}{d\tau} + \frac{dx_e}{d\tau}\right] &= \dot{m}_e - \dot{m}_f; \\ \varepsilon_c A_c\left[r_c\Phi'(\Theta_c)\frac{d\Theta_c}{d\tau} + \frac{dx_c}{d\tau}\right] &= \dot{m}_f - \dot{m}_c; \end{aligned} \qquad (5)$$

were the positive sign was accepted for: recessions in the direction into the bulk of wicks; evaporation from the evaporator and condensation on the condenser surfaces; liquid flow m_f in direction from condenser to evaporator.

The domain restricted by conditions:

$$\Theta' \le \Theta \le 0.5\pi; \qquad 0 \le x \le h_{wick}$$

These equations describe variations in interface

position due to alterations in liquid inventory and/or movement of mass of liquid.

The equation for liquid phase flow dynamic in a channel of variable geometry can be extracted from common momentum equation for uncompressed liquids:

$$\rho_l \frac{du_l}{d\tau} = \frac{\partial P}{\partial z} \tag{6}$$

In the assumptions of one-dimension flow the equation is:

$$a_1 \frac{d\dot{m}_f}{d\tau} = \frac{2\sigma \cos\Theta_e}{r_e} - \frac{2\sigma \cos\Theta_c}{r_c} - \frac{2\mu \dot{m}_f}{\rho} a_2 - (P_{ve} - P_{vc}) - \rho g(\tau) L_l \tag{7}$$

Where $g(\tau)$- gravity fluctuations.

The form factor a_1 is defined by integration along liquid flow direction Z from one interface to another one.

$$a_1 = \int_{x_e}^{L_t - x_c} \frac{dz}{A(z)} \tag{8}$$

The form factor a_2 is related to pressure losses in liquid paths.

$$a_2 = \int_{x_e}^{h_{we}} \frac{dz}{2A(z)\varepsilon_e K_e} + \int_{L_l}^{} \frac{S^2(z)dz}{A^3(z)} + \int_{L_t - h_{wc}}^{L_t - x_c} \frac{dz}{2A(z)\varepsilon_c K_c} \tag{9}$$

The integration limits depend of recession variables.

Change in curvature of menisci either causes liquid movement or withstands of pressure variation above the interfaces. Driving force for liquid path is created by a capillary pressure.

Momentum equation for vapor can be extracted by the same way.

$$a_1 \frac{d\dot{m}_v}{d\tau} = (P_{ve} - P_{vc}) - \Delta P_v(\dot{m}_v) \tag{10}$$

Driving force here is produced by pressure difference between vapor ducts of evaporator and condenser. Term ΔP_v includes components for pressure losses in vapor line, ducts and possibly in porous wicks.

The sound limit is controlled by the inequality

$$\dot{m}_v \le \frac{P_{ve}\pi D_v^2}{4} \sqrt{\frac{k}{R_v T_{ei}}} \tag{11}$$

Compressibility is partly accounted in the expression for pressure losses components along the vapor line, under assumption of linear low of pressure drop:

$$\Delta P_{Lv} = P_{v1} - \sqrt{P_{v1}^2 - \xi \frac{16\dot{m}_v R_v T_{ei} L_v}{\pi^2 D^5}} \tag{12}$$

Where P_{v1} – pressure at the inlet of the vapor line.

Terms of losses in porous elements in case of recession of interfaces can be expressed as following

$$\Delta P_{pve} = \frac{\mu_v \dot{m}_e}{\varepsilon_e K_e \rho_{v1}} \int_{-x_e}^{0} \frac{dz}{A_e(z)}; \qquad \Delta P_{pvc} = \frac{\mu_v \dot{m}_c}{\varepsilon_c K_c \rho_{v2}} \int_{-L_t}^{-L_t - x_c} \frac{dz}{\varphi_a A_c(z)}; \tag{13}$$

The integration limits also depends of recession variables. The integration takes place from external surface of evaporator wick up to one of condenser wick; the positive direction – along liquid path from 0 to L_t and the negative direction – along vapor path from 0 to $-L_t$.

The value φ_a is a rate of activity of the condenser, showing percentage of area which does not blocked with non-condensable gas.

For control volumes of vapor domains above the interfaces, variations of pressure follow the ideal gas low

$$\frac{dP_{ve}}{d\tau} = (\dot{m}_e - \dot{m}_v)\frac{R_v T_{ei}}{V_{ev}}; \qquad \frac{dP_{vc}}{d\tau} = (\dot{m}_v - \dot{m}_c)\frac{R_v T_{ci}}{\varphi_a V_{cv}}; \qquad P_g = P_{vc} \tag{14}$$

Mass flow rates of evaporation and condensation are expressed through the equations:

$$\dot{m}_e = \varepsilon_e A_e \frac{\alpha}{(1-0.4\alpha)} \sqrt{\frac{1}{2\pi R_v T_{ei}}} \cdot \left[P_{sat}(T_{ei}) - P_{ve}\right]; \qquad \dot{m}_c = \varphi_a A_c \frac{\alpha}{(1-0.4\alpha)} \sqrt{\frac{1}{2\pi R_v T_{ci}}} \cdot \left[P_{vc} - P_{sat}(T_{ci})\right]; \tag{15}$$

Where signs for the rates are positive if evaporation takes place on the evaporator and condensation – on the condenser.

In general case the position of the vapor-gas front defined from the bottom side of a reservoir can be found from the solution of integral equation

$$\int_0^{Y_i} \frac{\{P_{vc} - P_{sat}[T_i(y)]\}A(y)}{R_g T_i(y)} dy = m_g, \qquad (16)$$
$$\varphi_a = f(Y_i)$$

For the case of vapor channel of cylindrical shape the equation extracted from the model of Chi[2] can be applied

$$1-\varphi_a = \frac{R_g T_{cin}}{P_{gin} A_{cv}}\left[m_g - \frac{P_{gr} V_r}{R_g T_r}\right], \qquad (17)$$
$$P_{gin} = P_{vc} - P_{sat}(T_{cin}),$$
$$P_{gr} = P_{vc} - \delta_p P_{sat}(T_r)$$

Where δ_p=0 – for unwicked reservoir and δ_p=1 – for wicked reservoir.

Heat model is based on node technique. The evaporator zone is divided in three elements: grooved external wall, wick and liquid core.

Balance of the wall is determined by conduction from external surface to the interface, located in general case into the porous structure of the wick.

$$C_{ew} m_{ew} \frac{dT_{ew}}{d\tau} = Q_e(\tau) - G_{ewi}(T_{ew} - T_{ei}) \qquad (18)$$

Heat balance on the interface is defined by heat, coming from external wall; latent heat of vaporization; losses due to conduction through the wick from the interface to the liquid duct and heat, utilized for heating of liquid moving to the interface.

$$C_{ep} m_{ep} \frac{dT_{ei}}{d\tau} = G_{ewi}(T_{ew} - T_{ei}) - \lambda \dot{m}_e - \qquad (19)$$
$$- G_{ep}(T_{ei} - T_{el}) - \delta_f C_l \dot{m}_f (T_{ei} - T_{el})$$

Where δ_f=1 if $m_f \geq 0$ (i.e. liquid flows from condenser to evaporator) and δ_f=0 if m_f<0 (opposite direction).

The balance in liquid duct is determined by heat conduction through the wick and by specific heat of inlet and outlet liquid flows

$$C_{el} m_{el} \frac{dT_{el}}{d\tau} = (G_{ep} - \bar{\delta}_f C_l \dot{m}_f)(T_{ei} - T_{el}) \qquad (20)$$
$$+ \delta_f C_l \dot{m}_f (T_{elz} - T_{el})$$

Where T_{elz} –temperature of liquid on the outlet of the liquid line.

The external heat balance on the condenser is defined separately for active and inactive parts; the conduction between them also is taken into account

$$C_{cw} m_{cw} \varphi_a \frac{dT_{cw}}{d\tau} = G_{wi}(\varphi_a)(T_{ci} - T_{cw}) + \qquad (21)$$
$$\left(q_{ext}(\tau) - \varepsilon\sigma T_{cw}^4\right)\eta\varphi_a A_{cw} - G_{ain}(T_{cw} - T_{cin})$$

$$C_{cw} m_{cw} \varphi_{in} \frac{dT_{cin}}{d\tau} = G_{ain}(T_{cw} - T_{cin}) + \qquad (22)$$
$$\left(q_{ext}(\tau) - \varepsilon\sigma T_{cin}^4\right)\eta\varphi_a A_{cw}$$

The balance on the interface and in the liquid duct is similar to one for the evaporator:

$$C_{cp} m_{cp} \frac{dT_{ci}}{d\tau} = \lambda \dot{m}_c - G_{cp}(T_{ci} - T_{cl}) \qquad (23)$$

$$C_{cl} m_{cl} \frac{dT_{cl}}{d\tau} = (G_{cp} + \delta_f C_l \dot{m}_f)(T_{ci} - T_{cl}) \qquad (24)$$
$$- G_{ciw}(T_{cl} - T_{ci}) - \bar{\delta}_f C_l \dot{m}_f (T_{clz} - T_{cl})$$

Where T_{clz} –temperature of liquid at the inlet of the liquid line.

Important factor for overall modeling of CPL is time delay of liquid line. This factor is determined via the transport equation

$$A_l \rho_l \frac{\partial T}{\partial \tau} + \dot{m}_f \frac{\partial T}{\partial z} = 0 \qquad (25)$$

The node approximation of this equation gives the system of ordinary equation:

$$m_{lz} \frac{dT_{lz}^j}{d\tau} = \delta_f \dot{m}_f (T_{lz}^{j+1} - T_{lz}^j) - \qquad (26)$$
$$\bar{\delta}_f \dot{m}_f (T_{lz}^{j-1} - T_{lz}^j)$$

Where $j=1,,,n_z$ – number of nodes of liquid line.

For reservoir the equation will depend of the type of the reservoir.

Cold type reservoir:

$$C_r m_r \frac{dT_r}{d\tau} = q_{ext}(\tau) A_r - \varepsilon_r \sigma T_r^4 A_r \qquad (27)$$

Hot type reservoir:

$$C_r m_r \frac{dT_r}{d\tau} = G_r (T_{ew} - T_r) \qquad (28)$$

Insulated type reservoir

$$T_r = const$$

All these reservoir types follow the conception of passive control.

In the next sections the main results of the simulation of the base design of the CPL by the developed model is presented.

Hydrodynamic of dry-out

For purpose of better understanding of processes related with change of menisci curvature and interfaces movement, the hydrodynamic section of the model firstly was treated separately.

The interface movement has been simulated from initial position of x_e=x_c=1mm, without either evaporation or condensation. This case may be interpreted as insufficient charge.

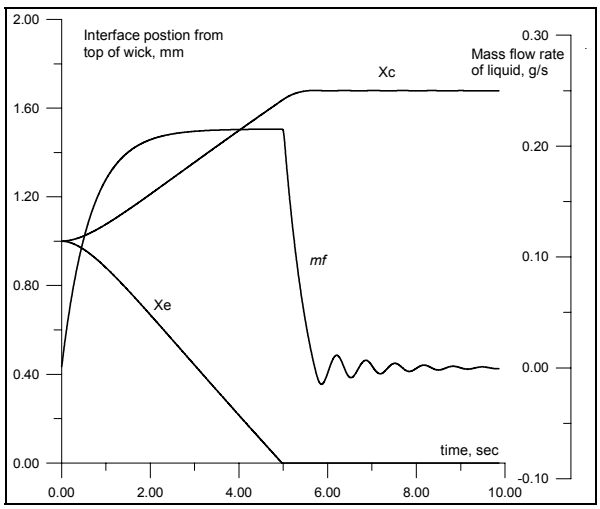

Fig. 4. A scenario of hydrodynamic stabilization before application of heat load, in conditions of charge deficit.

The mass flow rate is increased with deceleration, due to friction forces becomes more significant with velocity increasing. After the interface in the evaporator reaches the top surface of the porous structure, the liquid stops flowing with slight oscillation before complete stabilization.

The Fig. 5 shows the oscillation of wetting angle in evaporator with time for two diameters of liquid line. The initial positions of the vapor-liquid interfaces were as for the previous case (x_e=x_c=1mm) The length of liquid line between evaporator and condenser was accepted as long as 2m.

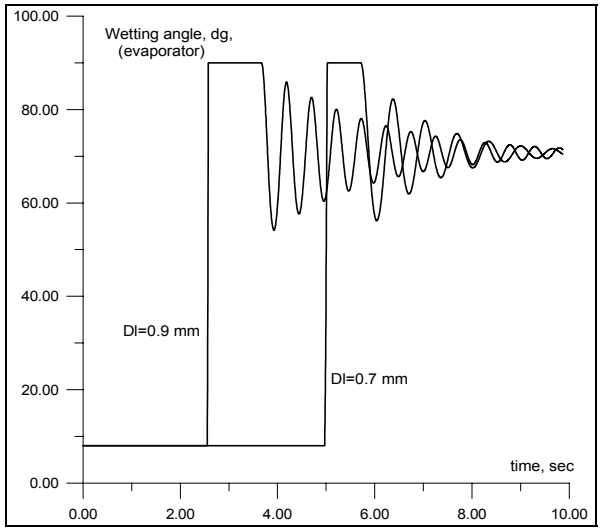

Fig. 5. Hydrodynamic of wetting angle stabilization for two diameters of the liquid line: 0.7 and 0.9 mm.

The frequency and amplitude of the oscillation depends on diameter, length of liquid line and liquid viscosity. Smaller diameter or long length of the liquid line damps the oscillation. Right shift on the graphic for case of 0.7 mm of liquid line is related to larger time delay for the liquid to reach the top surface of the wick with compare to the case of 0.9 mm.

A start-up scenario has been simulated by sudden application of 30 W heat load directly to the interface in the evaporator since of the instant of 2 s.

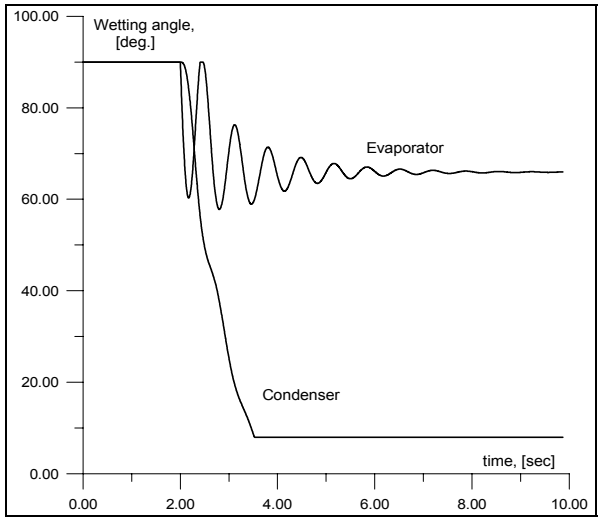

Fig. 6. Wetting angles behavior on idealized start-up.

Also it was accepted that condensation begins since the instant of 6 sec. This scenario simply imitates the case than initially condenser is blocked with non-condensable gas.

It was accepted that initially both the evaporator and condenser wicks are completely flooded by liquid (i.e. $\theta_e=\theta_c=90^0$)

The results are presented in the Fig. 6 The nonlinearity in profile of applied heat flux cause the micro-oscillation of the wetting angle θ_e , which can be observed on the picture. In reality the front of applied heat flux to the interface can not be flat.

The next picture (Fig.7) illustrates the reducing of the oscillation for the case, than the applied heat flux is being linearly increased to the maximum of 30 W during 1 sec since of instant of 2 sec. The inclined front was suggested for the condensation too. The condensation begins since the instant of 6 sec and linearly increased until the end time. The other initial conditions are the same as for the previous case.

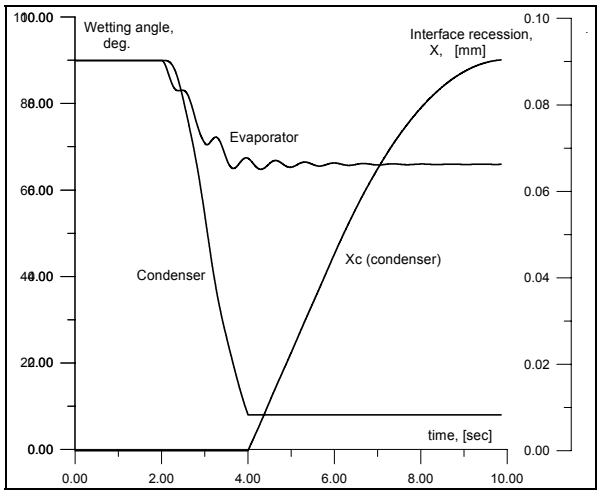

Fig.7. Wetting angle and interface recession propagation for the soft mode of heat load application on start-up.

This figure shows, that for nominal values of applied heat, hydrodynamic dry-out begins in the condenser wick, but not in the evaporator, due to the difference in the effective radii of pores. The curve of x_c tracks the interface recession in the condenser wick.

For the case of application of large amount of heat flux (200 W) with stiffer mode (during 0.5 sec), the sequence of events can be opposite. First, temporary dry-out occurs in evaporator and then - in the condenser. Next picture (Fig.8) shows the result of simulation for this case.

The extinguished character of oscillation of liquid mass flow rates around the rate of evaporation can be observed in the figure. Also the dynamic of the wetting angle θ_e is presented.

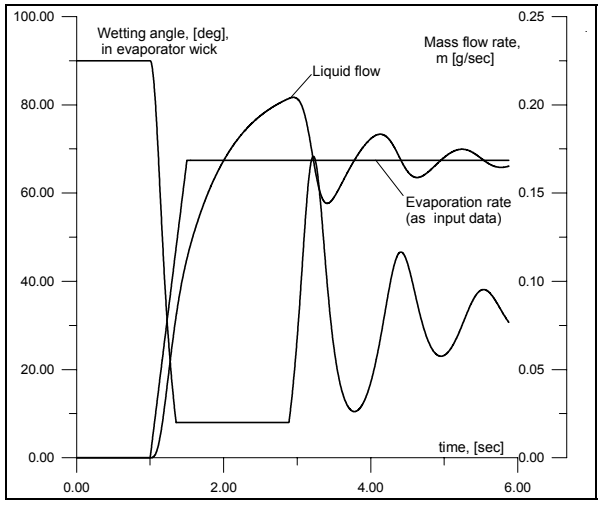

Fig.8. Stiff start-up with large heat flux.

The rate of partial fast initial dry-out in the evaporator wick depends of effective pore size of condenser wick. Next figure (Fig.9) exhibits the dynamic of evaporator interface propagation, calculated for different pore radii of condenser wick, during this stiff start-up (i.e. 200 W/ 0.5 sec since 2nd sec).

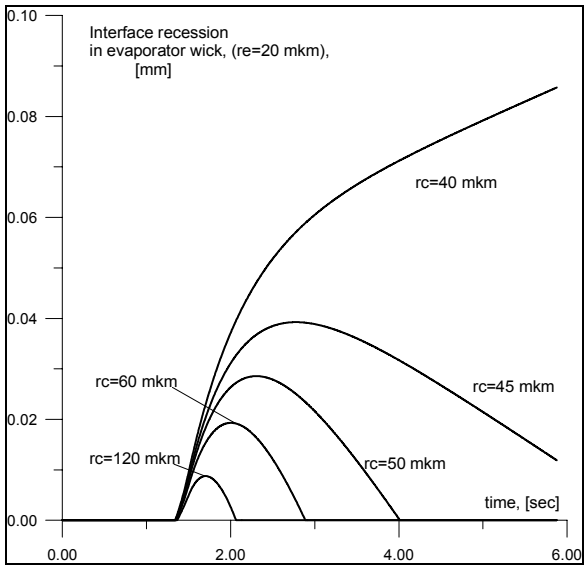

Fig.9. Evaporator interface recession propagation for different effective pore sizes of the condenser

The result shows that for this mode of start-up in conditions if the pore size in the condenser is close to one of evaporator (40μm and 20 μm respectively) the interval of partly dry-out of the evaporator can be significant

All graphics presented above display the results based on the hydrodynamic part of the model. Introduction of heat section of the model will smooth the transient oscillation due to thermal capacity. But, for critical regimes this hydrodynamic nonlinearity can appear. That is why important to leave this fast hydrodynamic section in the general model of CPL.

Vapor bubble formation conditions

Influence of thermal conductance of wick in the evaporator was studied. During the start-up, the heat dissipated at the upper side of the evaporator, is conducted through the porous wick and heats the liquid in the duct of the evaporator. It can cause the vapor formation under the internal surface of the wick. The large vapor bubble can interrupt the liquid supply to the wick and cause start-up failure. The amount of heat transferred trough the wick depends of thermal conductance of the wick and for poor conductivity wick the overheating of liquid can be less.

More, the liquid has to be subcooled, i.e. has to have lower temperature with compare to local saturation temperature, which depends of local pressure. The critical subcooling can be defined as the minimal temperature difference between the saturation temperature and temperature of the liquid.

The Fig.10 illustrates the dynamic of subcooling of the liquid with respect to local saturation temperature in the liquid in the duct located near the wick surface for the condenser.

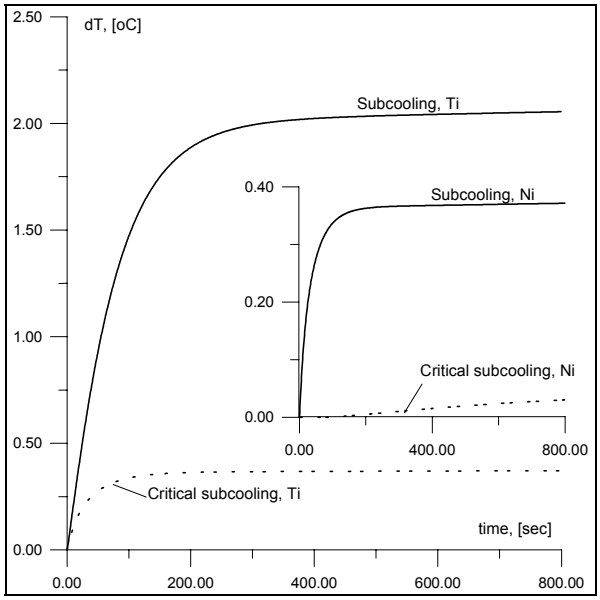

Fig.10. Predicted subcooling at the liquid duct of the condenser for different materials of the wick

The input data for this run was start-up from the uniform temperature of $+8.8^0$C with application of 30 W to evaporator and permanent conditions of condenser radiator under connate external heat flux of 120 W/m^2 . Material for both wicks is nickel powder.

The result on the Fig. 10 confirms that there are no conditions for vapor bubble formation during start-up in the condenser, because the predicted subcooling is constantly greater than critical one.

Next figure (Fig.11) shows the subcooling tracking for the same input data for the evaporator wick. Two cases treated: high-conductivity wick, made from nickel and poor conductivity wick, fabricated from titanium

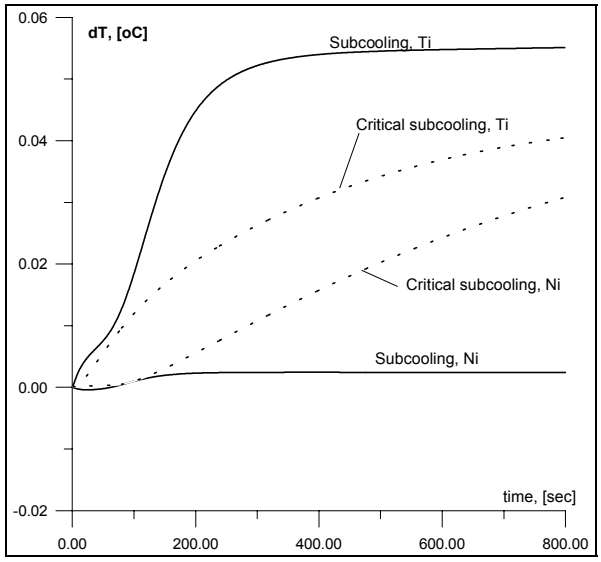

Fig.11. Predicted subcooling at the liquid duct of the evaporator for different materials of the wick

The result on the Fig.11 shows the favorable conditions of vapor bubble formation for the case of nickel wick during the start-up. It confirms the initial suggestion that the thermal resistance of the evaporator wick has to be high enough.

Next graph (Fig.12) displays behavior of subcooling conditions in evaporator for start-up from different initial temperatures, for Ti-wick.

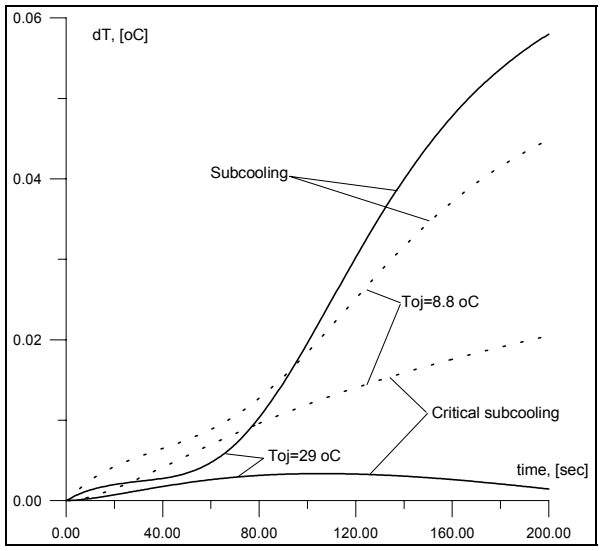

Fig.12. Subcooling variation in the evaporator under start-up from different initial temperatures.

For this case (Fig.12) safety conditions of prevention of bubble formation are satisfied continually during entire start-up.

Necessary subcooling depends of interface position in the condenser wick. If initially the interface will be partly recessed in the wick, the required subcooling should be more significant.

The next case for study is related to improper filling with liquid deficit. The Fig.13 shows a "subcooling insufficiency" dynamic for two different initial uniform temperatures for the start-up.

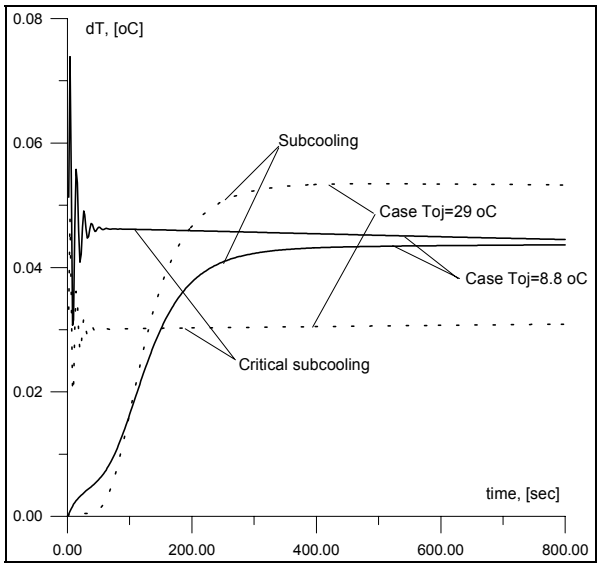

Fig.13. Subcooling transition under start-up from different initial temperatures in conditions of underfilling.

The result demonstrates that for "hot" start-up (T_{0j}=29^{0}C) there is initial period about of 140 sec of high probability of vapor formation. If the vapor bubble does not block the liquid supply to wick, it can collapse after, even without cold liquid feeding from the liquid line. In opposite case the complete dry-out of the evaporator wick can occurs.

For "cold" start-up (T_{0j}=8.8^{0}C) there are no conditions for the vapor bubble collapsing. Thus, for this combination of input data, the hot mode of the start-up is more reliable.

Modified initial data for this run was following: capillary recession of interface of 1 mm in the condenser and wetting angle of 90^0 in the evaporator. Other input data were the same as for previous cases of this section, for both titanium wicks.

The rate between subcooling and critical one for vapor prevention depends also of amplitude of applied heat flux on the start-up. The graphics on the Fig.14 illustrate these rates for 30 W (nominal mode) and 100 W (extensive mode) heat fluxes, applied to evaporator on start-up, from initial uniform temperature of -40^{0}C.

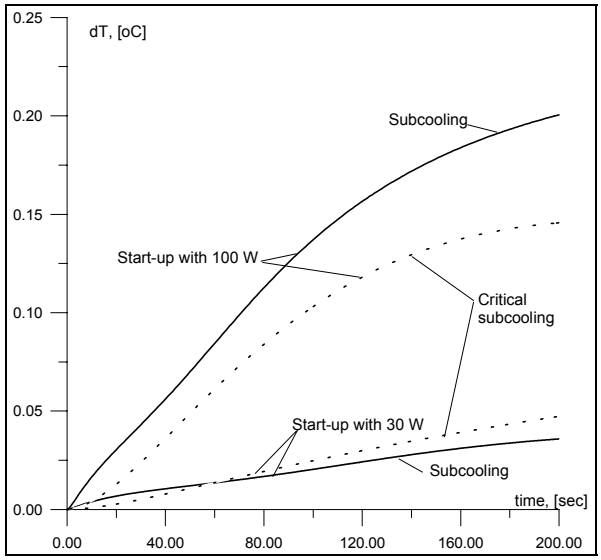

Fig.14. Subcooling transient under start-up with different heat loading

The result illustrates an interesting phenomenon when application of extensive load of 100 W during start-up may prevent of vapor bubble formation rather than application of nominal level of 30W.

Transient performance of the CPL

Transient characteristics of CPL in conditions without non-condensable gas were studied. Thermal capacity smoothes out the fast hydrodynamic nonlinearities, described above.

Next chart (Fig.15) displays start-up transition under normal mode of operation from initial uniform temperature of 0^{0}C and initial wetting angles of 90^0.

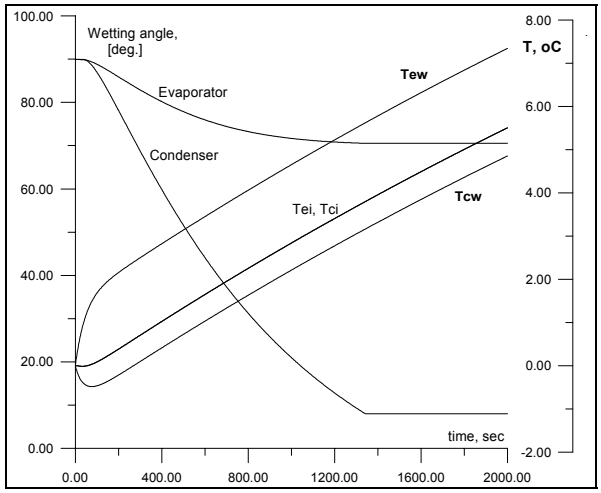

Fig.15. Start-up transient in normal mode with application of 30 W heat flux.

Phase transfer with combination of thermal capacity provide conditions for very slow transient processes in whole CPL. The time constant for entire

system can be of order of hours.

The heat flux profiles on the next graph (Fig.16) show the disbalance in condensed and radiated heat fluxes, which gives the conditions for long transient performance of the entire CPL. Heat load varies from 30 up to 45 W. Initial conditions: $T_{0j}=0^0C$ and $T_{0j}=30^0C$.

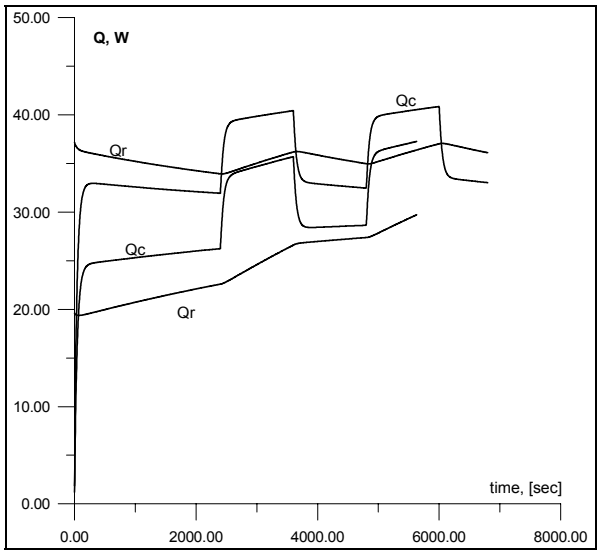

Fig.16. Heat fluxes of condensation and radiation on the condenser, for two different initial conditions

The temperature profiles for these cases are shown in the Fig.17.

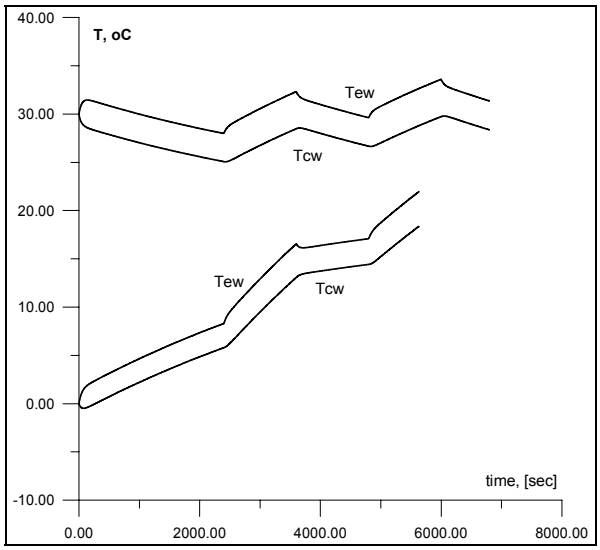

Fig.17. Temperature profiles for different initial conditions

The overall temperature difference : (Tew-Tcw) is approximately constant for every heat load: 3.0^0C for Q=30 W and 3.8^0C for Q=45 W. The estimated time to reach steady-state conditions is about 3 hours.

Farther study of transient performance was conducted for the case of cooling after completely switch-off heat load of 30 W after 300 sec of the operation. External flux is constant: 120 W/m^2.

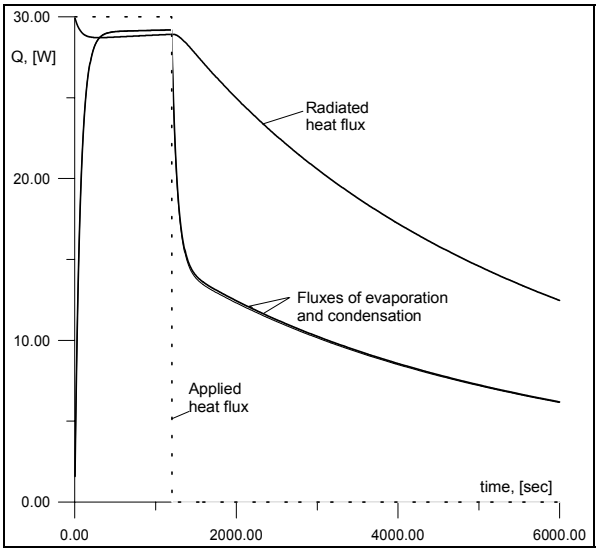

Fig.18. Cooling transient process in the CPL after switch-off heat load.

The cooling curve gives impression about thermal capacity performance of entire system without presence of non-condensable gas.

Below the temperatures on external surfaces on evaporator and condenser walls are presented for the same case.

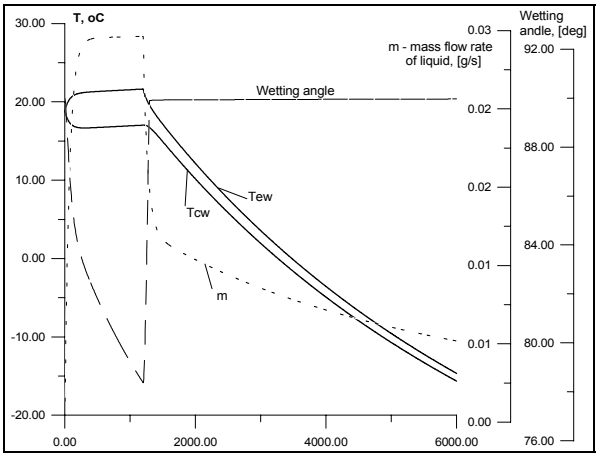

Fig.19. CPL parameters transition during cooling after switch-off heat load.

Wetting angle is changed in respond of applied heat. After switch-off his value becomes slight less than 90^0C, just enough to pump liquid of reduced mass flow rate.

The curve of positive mass flow rate demonstrates ability of the system to operate without application of heat load on evaporator, but just due to cooling from the radiator side.

Model of control

The next set of modeling results is related to simulation of gas-loaded modes of operation of the CPL.

The Fig.20 shows the result for the same case of cooling after completely switch-off heat load of 30 W after 300 sec of the operation. The type of the reservoir is insulated one with initial temperature of 20^0C.

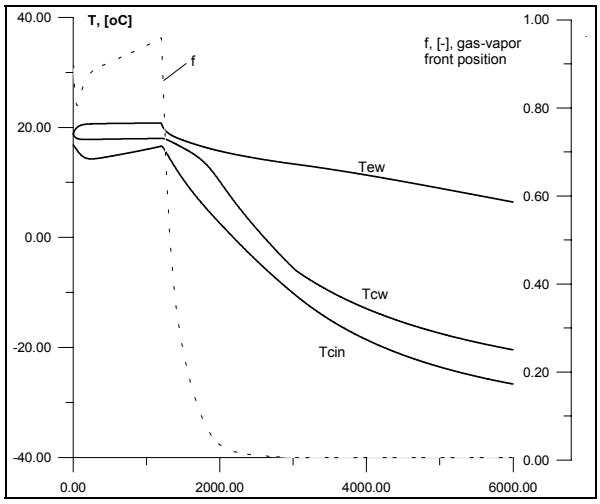

Fig.20. Cooling transient process in the gas-loaded CPL after switch-off heat load.

The input data for this run was exactly the same as for the case, presented in the Figures 18-19. The comparison these results demonstrates ability of self-control of the gas-loaded (GL) CPL. For the case of ordinary CPL the temperature of the evaporator falls down to -15^0C, but for GL system - down to $+7^0$C. Also the curve of the vapor-gas front tracking shows that the condenser has been practically blocked since about 2000 sec of current time of the process.

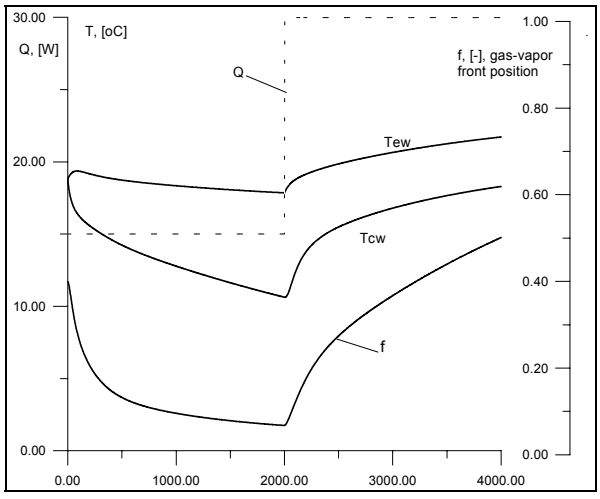

Fig.21. Transient performance and front tracking in the GL CPL with insulated reservoir.

Next run (see Fig.21) has been done to demonstrate the transient performance of GL CPL when heat load on the evaporator is switched from 30 W up to 45 W. External flux is constant: 120 W/m^2.

One can see the relatively stability of evaporation temperature (Curve T_{ew}, Fig.21).

The Fig. 22 shows the obtained result for two simulations of transient processes in the gas-loaded and ordinary CPL of the same geometry under identical conditions. The sequence of loading was following: 15W-0W-30W-15W.

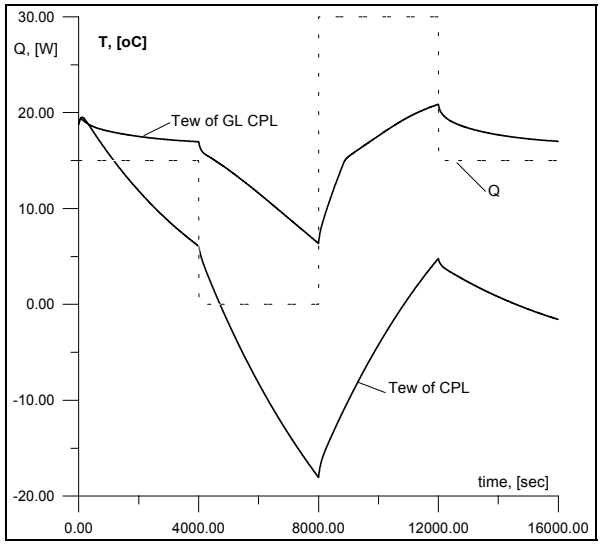

Fig.22. Comparative analysis for ordinary and GL CPL with insulated reservoir.

The relative stability of evaporator wall temperature is observed.

Various conceptions of reservoir type have been examined in the following study.

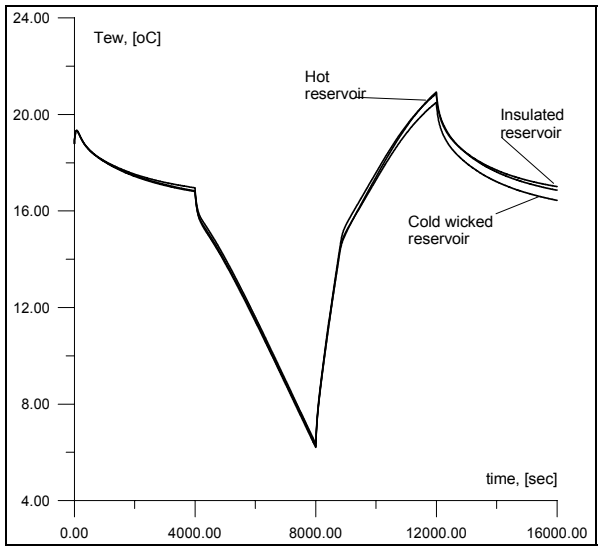

Fig.23. Comparative analysis for different types of the gas reservoir

The Fig. 23 shows final result of modeling the GL CPL with different types of reservoir under the same input conditions, used in the former study. The types include the unwicked insulated, wicked cold and unwicked hot ones.

The gas/vapor front position variation for this case is presented in the Fig. 24.

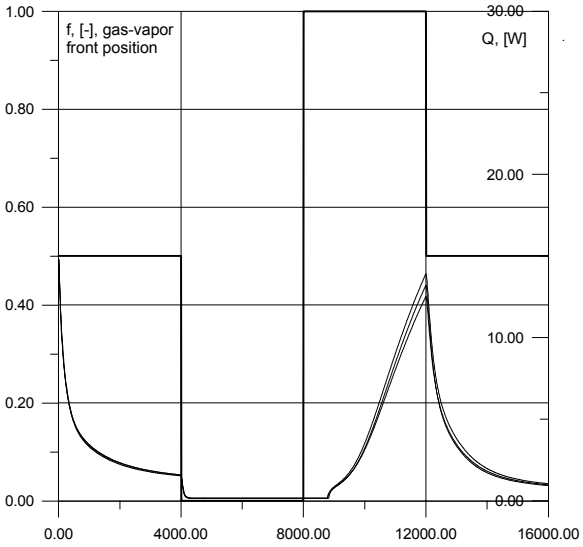

Fig.24. The vapor-gas front tracking for three types of the gas reservoir.

One can observe no distinguished differences exist in the CPL parameters excursion for all types of examined reservoirs

The Fig. 25 shows the obtained result for two simulations of transient processes in the gas-loaded and ordinary CPL of the same geometry under conditions when heat flux applied to the evaporator is constant (Q=30W), but the external heat flux, impacting on the condenser radiator, is variable.

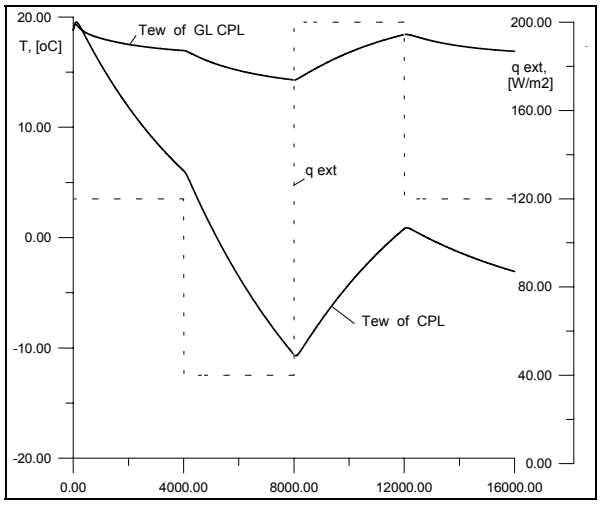

Fig.25. Comparative analysis for ordinary and GL CPL for the case of variable external heat fluxes.

The external flux was varied with according to the scheme: 120-40-200-120 W/m^2.

The Fig. 26-27 show the result of simulation for the former case of the variable external heat fluxes for the different types of reservoir

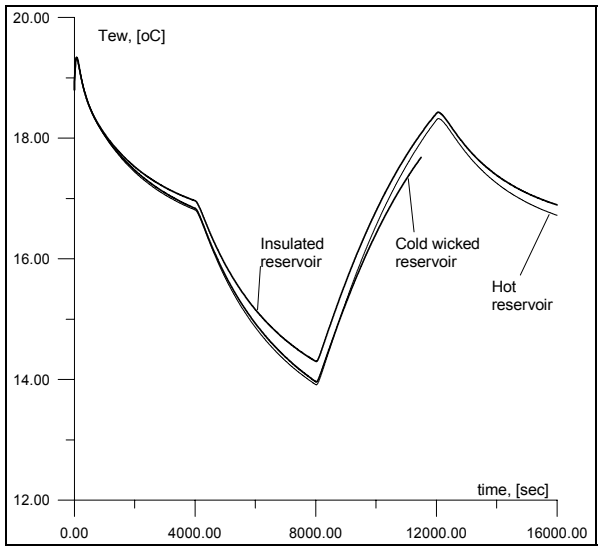

Fig.26. The evaporator temperature profiles for different types of the gas reservoir for the case variation of external conditions on the condenser.

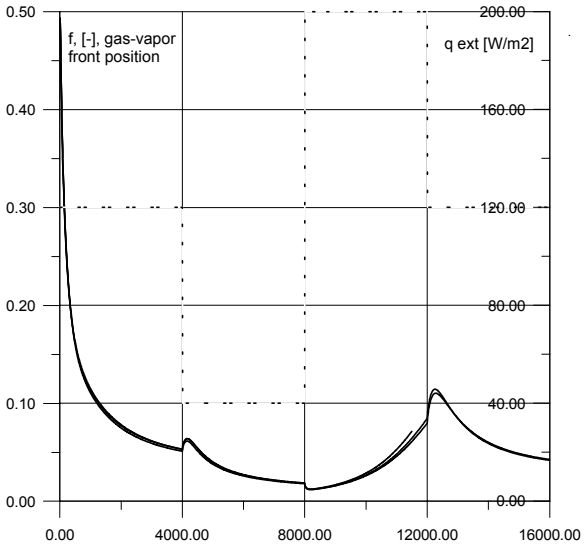

Fig.27. The vapor-gas front tracking for three types of the gas reservoir for the case variation of external conditions on the condenser.

Finally, it can be concluded, that the transient behavior of self-control for gas-loaded CPL is similar to that for a VCHP.

Conclusion

The proposed CPL with wicked condenser and passive control with non-condensable gas can represent a competitive alternative of existing capillary pumped loops. This theoretical examination of the conceptual model of variable conductance CPL confirms possibility to develop a high performance self-controlled heat transport system with wicked condenser. Fixing a vapor/liquid interface with the porous structure in the condenser gives several advantages, compared to the traditional tube type condenser design.

The developed model gives representative description of all main conjugate hydrodynamic and heat transient processes in the whole GL CPL.

Acknowledgments

This research was conducted at INPE under partial support of Brazilian Foundation of Science and Technology - CNPq, and Foundation of Research Support of Sao Paulo State - FAPESP.

References

1. Bazzo, E., Colle, S., 1995, "Bombas capilares aplicadas a circuitos de transferência de calor de dupla-fase". *XIII Congresso Brasileiro e II Congresso Ibero Americano de Engenharia Mecânica*, Belo Horizonte, Brazil, December 12-15.
2. Chi, S.W., "Heat Pipe Theory and Practice a Source Book". Hemisphere Publishing Corp., McGraw-Hill Book Company, 1976.
3. Dickey, J.T., and Peterson, G.P., 1993, "An Experimental and Analytical Investigation of the Operational Characteristics of a Capillary Pumped Loop", AIAA Paper 93-2746.
4. Furukawa, M., 1996, "Methods and Analysis for Capillary Pumped Loop Pressure/Temperature Control," *Proceeding, 31st AIAA Thermophysics Conference*, June 17-20, 1996/ New Orleans, LA, AIAA paper 96-1831, pp. 1-23.
5. Faghri, A., 1995*, "Heat Pipe Science and Technology*". Taylor&Franis.
6. Gottschlich, J.M. and Richter, R., 1991, "Thermal Power Loops", SAE 91-1188, *Proc. SAE Aerospace Atlantic,* Dayton, OH.
7. Hoang, T.T., Ku, J., 1995, "Theory of Hydrodynamic Stability for Capillary Pumped Loops", *Proceeding, HTD-Vol.307, 1995 National Heat Transfer Conference* - Volume 5 /ASME, pp. 33-40
8. Ku, J. "Performance tests of CAPL2 starter pump cold plates", *31st AIAA Thermophysics Conference*, New Orleans, LA, June 17-20, 1996.
9. Ku, J., Hoang, T.T., 1995, "An Experimental Study of Pressure Oscillation and Hydrodynamic Stability in a Capillary Pumped Loop*", Proceeding, HTD-Vol.307, 1995 National Heat Transfer Conference* - Volume 5 /ASME, pp. 25-32
10. Maidanik, Y.F., et.al., 1992, "Thermoregulation of loops with capillary pumping for space use". *Proceedings, 22nd International Conference on Environmental Systems,* Seattle, Washington, July 13-16.
11. Maidanik, Y.F., Fershtater, Y.G., Goncharov, K.A., 1991, "Capillary Pump Loop for the Systems of Thermal Regulation of Spacecraft". *Proceedings, 4th European Symposium on Space Environmental and Control System,* Florence, Italy, October 21-24.
12. Meyer, R.; et al. "Investigation of the heat transfer performance of a capillary pumped ammonia loop under gravity", *23rd International Conference on Environmental System*, Colorado Springs, Colorado, July 12-15, 1993.
13. Ochterbeck, J.M., "Modeling of Room-Temperature Heat Pipe Startup from the Frozen State", *AIAA Journal of Thermophisics and Heat Transfer,* Vol. 11, No 2, pp. 165-172.
14. O'Connell, T., Hoang, T., Ku, J., 1996, "Effects of Transport Line Diameters on Pressure Oscillations in a Capillary Pumped Loop", *Proceeding, 31st AIAA Thermophysics Conference*, June 17-20, 1996/ New Orleans, LA, AIAA paper 96-1833, pp1-5.
15. Peterson, G.P., 1983, "Two phase thermal control systems for spacecraft instrumentation", *AIAA 18th Thermoph. Conf.,* Montreal, Canada, June 1-3.
16. Stenger, F.J., 1966, "Experimental Feasibility Study of Water-Filled Capillary Pumped Heat Transfer Loops", Technical Report NASA X-1310.
17. Tournier, J.-M., El-Genk, M.S., 1994, "A Heat Pipe Transient Analysis Model," *Int. J. Heat Mass Transfer*, Vol. 37, No. 5., pp. 753-762.
18. Tournier, J.-M., El-Genk, M.S., 1996, "A Vapor Flow Model for Analysis of Liquid-Metal Heat Pipe Startup from a Frozen State," *Int. J. Heat Mass Transfer*, Vol. 39, No. 18., pp. 3767-3780.
19. Vlassov, V.V., Muraoka, I., 1996, "Experimental examination of a prototype of the capillary pumped loop with porous condenser", *Proceeding: VI Congresso Brasileiro ENCIT/LATCYM*, Florianópolis SC, Brasil, 11-14 de novembro 1996, Vol. 2, pp. 883-888.
20. Wulz, H.G., Mayinger, F., 1992, "Heat and fluid transport in an evaporative capillary pump", *International Journal of Energy Research,* Vol.16, pp. 879-896.